J. Fluid Mech. (1978), *vol.* 89, *part* 3, *pp.* 413–432
Printed in Great Britain

Large-scale structure in the mixing layer of a round jet

By A. J. YULE

Department of Chemical Engineering and Fuel Technology,
University of Sheffield, England

(Received 16 June 1977 and in revised form 2 March 1978)

Late transitional and turbulent flows in the mixing-layer region of a round jet are investigated for a range of Reynolds numbers by using flow-visualization and hot-wire techniques. Attention is focused on the vortices in the transition region and the large eddies in the turbulent region. The interaction and coalescence of vortex rings in the transition region are described. The transition region is characterized by a growth of three-dimensional flow due to a wave instability of the cores of the vortex rings. The merging of these distorted vortices produces large eddies which can remain coherent up to the end of the potential-core region of the jet. A conditional sampling technique is used to measure eddies moving near the jet centre-line. These eddies differ significantly from the ring vortices as they are three-dimensional and contain irregular small-scale turbulence. However, when averaged, their structure is similar in cross-section to that of a vortex ring. These sampled eddies contribute greatly to local velocity fluctuations and statistical correlations. The experiments indicate a need for careful consideration of the meanings of terms such as 'vortex', 'eddy' and 'turbulent flow'. In particular care must be taken to discriminate between the orderly, easily visualized, vortices in the transition regions of free shear flows and the less clearly visualized, but strong, large eddies in the fully developed turbulent regions.

1. Introduction

This investigation has the objective of obtaining a clearer understanding of the physical nature of the large-scale structure in the mixing-layer region of a round jet. Free jets developing from thin laminar nozzle boundary layers are considered, with the notation shown in figure 1. The initial instability of the laminar shear layer near the nozzle is well understood both analytically and experimentally; see Michalke & Freymuth (1966) and Wille (1963) respectively, for example. For all but the lowest Reynolds numbers, when other instability modes can occur, this instability results in a migration of vorticity to form periodic, circumferentially coherent concentrations in the shear layer. This has the physical appearance of the rolling-up of the laminar shear layer to form a periodic street of vortex rings. The mechanisms by which these vortices break down into turbulent flow are not clearly established.

Measurements in the turbulent region of the mixing layer have been made in many investigations by hot-wire techniques and these investigations have often indicated the importance of the large eddies in the turbulent flow. Certain experimental results, obtained by conditional sampling and flow visualization techniques, have been used to infer that these eddies are similar to the vortex rings formed from the initial

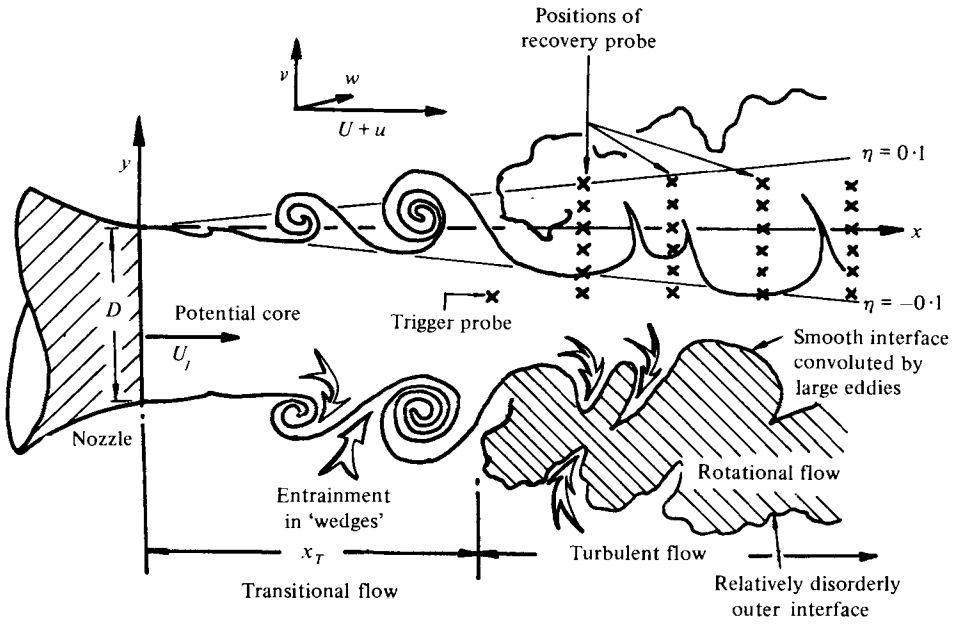

FIGURE 1. Notation for round free jet.

instability. Examples of these investigations are the conditional sampling experiments by Lau & Fisher (1975) and the flow-visualization studies by Crow & Champagne (1971). However, Davies & Yule (1975), and others, have pointed out that the evidence supporting the existence of vortex rings in the turbulent jet, as opposed to the jet transition region, is not conclusive. Thus flow visualizations which demonstrate the presence of vortex rings do not generally prove that the region in which these rings are found is fully turbulent. In addition, although certain features of the data from conditional sampling experiments in the turbulent mixing layer may be consistent with those expected for classical vortex rings, other features of the data are not. It has been argued, for example by Laufer (1973), that the basic flow in a turbulent round jet consists of a street of interacting and coalescing vortex rings. Other recently published experimental work, e.g. Moore (1977), has discussed the turbulent flow in terms of vortex rings.

It is considered that the use of the terms 'vortex ring' or 'vortices' to describe structures in the turbulent region can lead to confusion and that the terms 'eddy' or 'large eddy' are preferable unless the presence of such vortex rings has been firmly established. To a certain extent the difficulty is one of semantics and it is useful at the outset to establish the meanings of these terms when they are used to describe flow structures. Thus *vortex* is assumed to have the received meaning, implied by classical vortex rings and line vortices, of the flow field accompanying a concentrated, continuous, coherent distribution of vorticity which is uniform in the direction of the vorticity vector and which grows in scale by viscous diffusion alone. The term eddy has usually been used in the past in a far more general sense than the term vortex. Thus an *eddy* may be described as a vorticity-containing region of fluid which can be identified as moving as a coherent structure in a flow. Thus at one extreme of order-

liness, a large eddy in a flow may be a vortex ring and at the other extreme the term can be used to describe a perhaps rather weak and transient large-scale coherence imposed on a wide range of more energetic smaller scales of turbulence. The present results described below confirm the correlation data of Bradshaw (1966), which indicate that large eddies in the turbulent region have structures which lie between these two extremes. These eddies are indeed very important features of the turbulent flow and they may remain coherent for a significant downstream distance, however features such as their three-dimensionality and the irregularity of the vorticity fields within them precludes the use of the term vortex ring to describe them.

Interest in the roles of large eddies in free shear flows intensified following the flow-visualization studies by Brown & Roshko (1971, 1974) and Winant & Browand (1974) of two-dimensional mixing layers. Strong, clearly visible, line-vortex-like large eddies were found, which grew in scale by coalescing with their neighbours. In an investigation contemporary with the present experiments, Chandrsuda *et al.* (1978) reported results which support comments on the flows studied by Roshko and Browand which were made by Davies & Yule (1975) and Bradshaw (1975). Thus the earlier Roshko or Browand experiments appear to represent mixing layers which are not fully turbulent and in which the coherent line-vortex eddies are not representative of the strong, but less orderly and fully three-dimensional eddies which exist in the fully developed turbulent state. In later experiments Dimotakis & Brown (1975, 1976) and Konrad (1976) indicated that the mixing layers do develop three-dimensional eddy structures, with substantial smaller-scale turbulence, at higher Reynolds numbers and at the end of the test rig, but they concluded that the coherence of the large-scale features was not destroyed by this development.

The first stages of this investigation were reported by Yule *et al.* (1974) and Davies & Yule (1975). It was described how the transition to turbulent flow involved a relatively orderly three-dimensional deformation of the initial vortex rings and a growth of randomness in the vortex movements. Browand & Laufer (1975) carried out a very similar series of experiments with results which agreed closely with those of Yule *et al.* Browand & Laufer considered that the turbulent jet contains interacting turbulent (thick-cored) forms of the initial vortices, which, as suggested by Yule *et al.* (1974), may be similar to the vortex rings studied by Maxworthy (1974). This paper gives a fuller account of the work described by Yule *et al.* for a wider range of Reynolds numbers and examines the structures of the turbulent eddies. The mechanism of breakdown of the vortex street and the connexions, similarities and differences between the large eddies and the vortices are discussed. This investigation has resulted in an emphasis on the differences between the turbulent large eddies and the early rings and it is pointed out that it is dangerous to oversimplify the turbulence structure by thinking in terms of interacting vortex rings. The findings are closely paralleled by the observations by Chandrsuda *et al.* (1978) comparing the structures of eddies in turbulent and transitional two-dimensional mixing layers.

The investigation studies the transitional and turbulent flows for a range of Reynolds numbers. To ensure the accurate interpretation of observed structures it was necessary to make sufficient point velocity measurements to demonstrate conclusively, within acceptable criteria, the local transitional or turbulent nature of the flow. It is thus necessary to define criteria to distinguish between turbulent and non-turbulent regimes. In the absence of a universally accepted definition of turbulence it is not

possible to define criteria which are applicable to all turbulent shear flows. In practice it is clear for the round jet whether local velocity time histories are associated with turbulent or transitional flow as is described below.

2. Turbulent and transitional flow: discrimination by point measurements

Point measurements of the mean and fluctuating velocity components were made in the mixing-layer region of an air jet issuing from a 50·8 mm diameter nozzle for a range of jet Reynolds numbers: $9000 \leqslant Re \leqslant 2 \times 10^5$, where $Re = U_j D/\nu$ and U_j is the jet exit velocity. Cross-wires were used, with constant-temperature anemometers and analog linearizers. Data were either processed in real time, by using a Hewlett–Packard Correlator, or were stored and subsequently processed by using a data-analysis computer. These experiments provide information on the locations of transitional and turbulent regions in the jet to aid the interpretation of flow-visualization and conditional sampling experiments. In addition they provide systematic data on jet transition as a function of Re.

Initial experiments showed that the mean velocity profile achieved its characteristic turbulent 'error function' shape in the mixing layer very near the nozzle and considerably before the local fluctuating velocity signals were turbulent in form. This is also found in the results of previous experiments on the transition of round jets and two-dimensional mixing layers, for example the experiments of Wille (1963) and Yule (1972) respectively. Thus the existence of a similarity form for the mean velocity profile cannot be used as a sole criterion for proving that fully developed turbulent flow exists locally. Characteristics of the fluctuating velocity field were measured to discriminate between transitional and turbulent regions.

Figure 2 shows the distributions of the radial and circumferential intensity components $(\overline{v^2})^{\frac{1}{2}}$ and $(\overline{w^2})^{\frac{1}{2}}$ along $\eta = 0$ for different Re. The distributions have basic similarities for all Re. $(\overline{v^2})^{\frac{1}{2}}$ increases to a peak near the orifice then decreases more slowly to the nearly constant value found in the fully developed turbulent mixing layer and $(\overline{w^2})^{\frac{1}{2}}$ increases gradually to its turbulent value, which is reached at a similar distance downstream. The $(\overline{u^2})^{\frac{1}{2}}$ component increases rapidly to reach its turbulent value considerably before the other intensity components.

For a particular value of Re the asymptotic turbulent values of the three intensity components were the same to within 15 %. The turbulent values of $(\overline{u^2})^{\frac{1}{2}}/U_j$ varied between 0·14 and 0·15 in the range of Re investigated, thus indicating the existence of Reynolds number similarity. The value of x at which both $(\overline{v^2})^{\frac{1}{2}}$ and $(\overline{w^2})^{\frac{1}{2}}$ are within 5 % of their turbulent values is plotted in figure 3. This is one possible definition of the transition distance x_T.

Measurements of the Reynolds shear covariance $\overline{uv}(\tau)$ with a time delay τ were made for the same jets. The measurements for $Re = 21\,000$ shown in figure 4 are typical of the trends found. There is a transition from a periodic correlation near the nozzle, where u and v are almost in quadrature, to a cusp-shaped correlation at $x = 4D$ which is indicative of significant high frequency components and is characteristic of low intermittency regions of turbulent shear flows. The shape of the latter turbulent distribution is retained downstream throughout the turbulent jet (in low intermittency regions). This distribution is also found in the turbulent regions for all

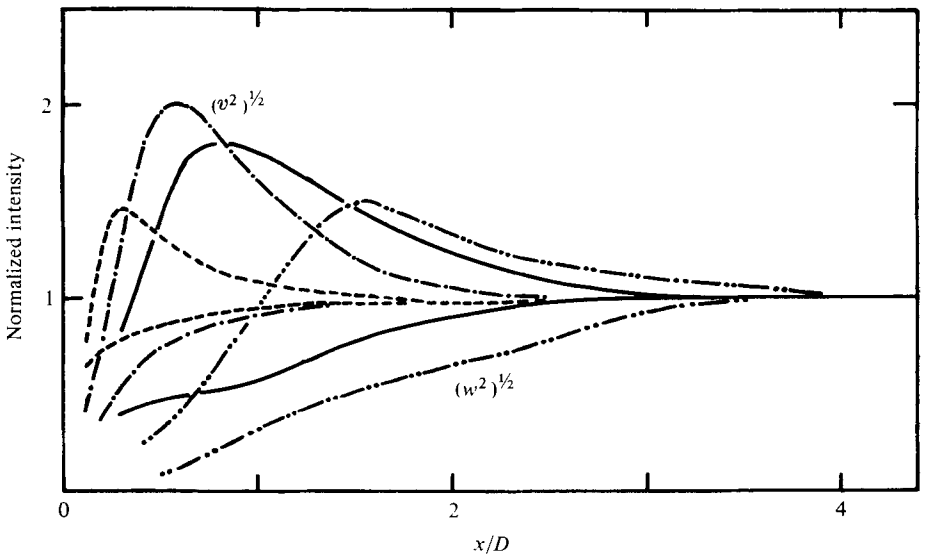

FIGURE 2. Longitudinal distributions of intensity components at $\eta = 0$ as a function of Re, normalized by values at $x = 4D$. ··—··, $Re = 9 \times 10^3$; ——, $Re = 3{\cdot}5 \times 10^4$; · —· —·, $Re = 5 \times 10^4$; – – – –, $Re = 10^5$.

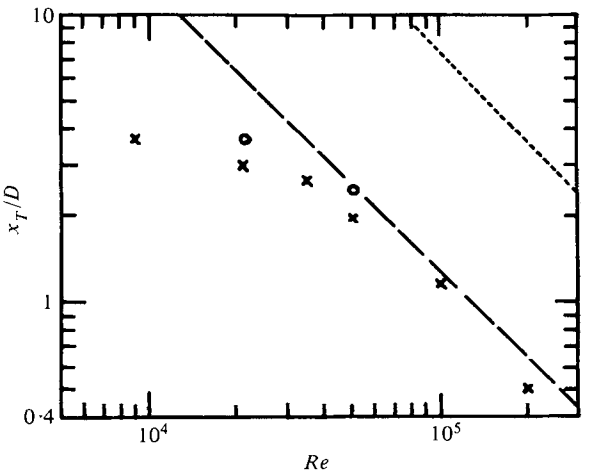

FIGURE 3. Transition distance as a function of Re in air jet. ×, from intensity data; ○, from covariance data; ———, $x_T U_j/\nu = 1{\cdot}2 \times 10^5$; – – – –, $x_T U_j/\nu = 7 \times 10^5$.

the values of Re and scales on local velocity and length scales. The covariances of other fluctuating quantities, e.g. $\overline{uu}(\tau)$, change at similar rates from periodic forms near the nozzle to their characteristic fully developed forms. The transitional jet flow ends when these turbulent forms of the covariances (or spectra) are established and values of x_T estimated from these measurements are included in figure 3. It is seen that this definition gives values of x_T which are typically $0{\cdot}25D$ larger than values based on the measurements of $(\overline{v^2})^{\frac{1}{2}}$ and $(\overline{w^2})^{\frac{1}{2}}$. However one can reasonably assume that the jet mixing layer is locally turbulent when the peak values of $(\overline{v^2})^{\frac{1}{2}}$ and $(\overline{w^2})^{\frac{1}{2}}$ are within 15% of each other and independent of x. It was concluded that the

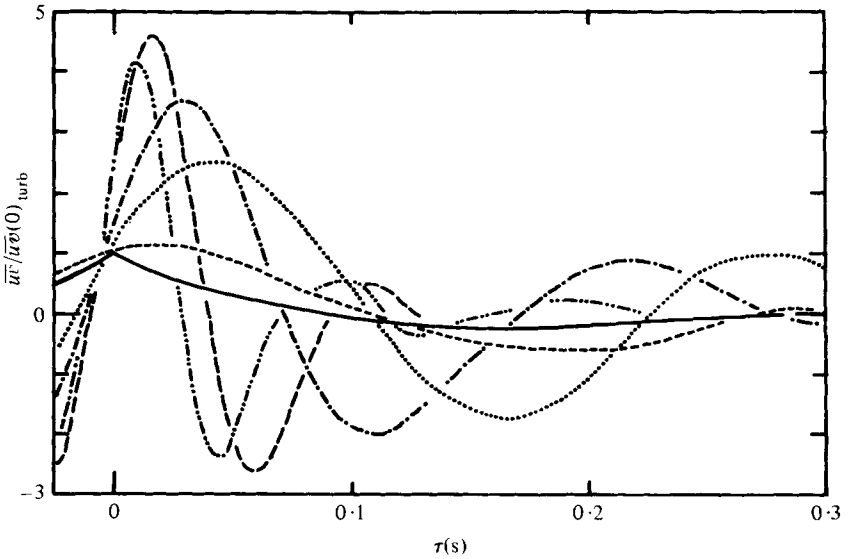

FIGURE 4. Shear-stress covariance with time delay at $\eta = 0$ for $Re = 2{\cdot}1 \times 10^4$. ··—··, $x/D = 0{\cdot}5$; ————, $x/D = 0{\cdot}75$; ·—·—·, $x/D = 1{\cdot}5$; ·····, $x/D = 2{\cdot}5$; – – – –, $x/D = 3{\cdot}5$; ——, $x/D = 4$.

attainment of similarity distributions of $(\overline{u^2})^{\frac{1}{2}}$ and U across the mixing layer (and also the attainment of a constant rate of spread for the mixing layer) could not be used as criteria for proving the local existence of fully developed turbulent flow. Bradshaw (1966) suggested that the assumption of a constant transitional Reynolds number $x_T U_j/\nu \simeq 7 \times 10^5$ may provide a reasonable estimate of x_T for his experiments. It can be seen from figure 3 that $x_T U_j/\nu = 1{\cdot}2 \times 10^5$ gives reasonable agreement with the present data.

The fully developed turbulent mixing layer and the transition region are thus distinguishable by the fully three-dimensional structure of the turbulent flow and the similarity forms of the correlation functions which are found in the turbulent flow.

3. Vortex rings in transition region

3.1. *Air jet*

The periodic, quadrature shapes of the correlations in figure 4 indicate the presence of vortex rings in the transition region. Bradshaw (1966) has described how peaks in $\overline{u^2}$ and $\overline{v^2}$ intensity distributions near the nozzle may be related to the coalescing of these vortex rings. These vortex rings can also be related to peaks in velocity frequency spectra measured in the jet potential core. Figure 5 shows u power spectra P_u for $Re = 21\,000$ for different x along the line $\eta = 0{\cdot}15$, which is in the jet potential core near the inner edge of the mixing layer. The measurements for $x = 4D$ and $x = 5{\cdot}5D$ were made on the jet centre-line as $\eta = -0{\cdot}15$ crosses the centre-line at $x = 3{\cdot}33D$. It is seen that as x increases frequency halving occurs in the spectra.

High-speed ciné films of the various jets were made with visualization by use of smoke injection in the jet settling chamber and a narrow beam of light from a slit

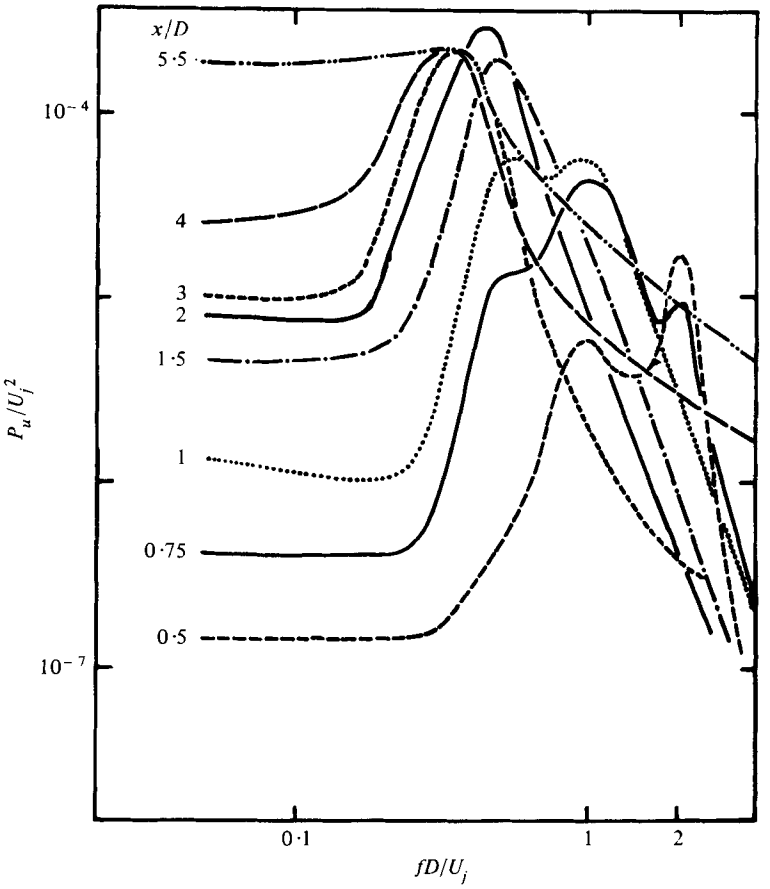

FIGURE 5. Power spectra of u at $\eta = -0{\cdot}15$ for $Re = 2{\cdot}1 \times 10^4$.

source 10 mm wide. The vortex rings could be clearly seen in these films in the regions where frequency halving was found in the spectra. The average local passing frequencies of the vortices were measured from these films and these measurements were always within 5 % of the local P_u spectra peaks. Vortex coalescing could also be clearly seen in these films and, as expected, the average positions where coalescence occurred were the same as the positions where frequency halving was observed in the spectra. The coalescing of neighbouring vortex rings is similar to that observed for line vortices in two-dimensional mixing layers and involves engulfment of potential-flow fluid in wedges between the vortices.

The distributions of the Strouhal numbers $St(x) = FD/U_j$ derived from the u spectra are shown in figure 6 for three values of Re, where F is the peak frequency. Examination of the ciné films of the jets combined with the spectral measurements and the knowledge of the locations of the transitional and turbulent regions yielded the following qualitative observations about the transitional flow.

(i) Ring vortices are not observable in the turbulent regions of the jets.

(ii) Peak-frequency halving, associated with coalescence, does not occur in the turbulent region.

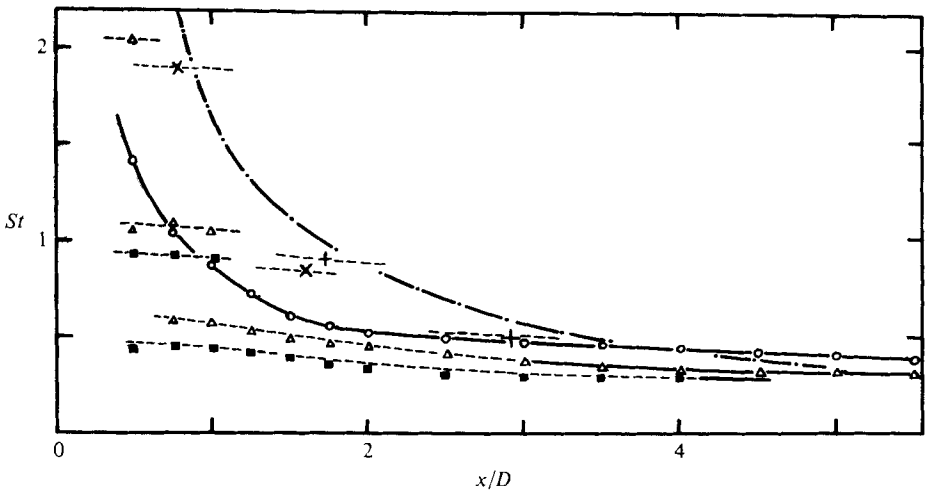

FIGURE 6. Strouhal numbers calculated from potential-core u spectra peaks in air jet and average vortex passing frequencies in water jet. Re of air jet: ■, $7{\cdot}1 \times 10^3$; △, $2{\cdot}1 \times 10^4$; ○, 2×10^5. Re of water jet: ×, $1{\cdot}2 \times 10^4$; +, $4{\cdot}5 \times 10^3$. ——, turbulent regime; – – – –, transitional regime.

(iii) The transitional flow can contain up to three vortex-coalescing regions depending on Re.

(iv) These regions overlap in a given jet, i.e. there are no fixed values of x at which coalescence always occurs.

(v) The initial orderly, spiral interface between the jet and the entrained ambient fluid in the vortex becomes increasingly disordered and diffuse as coalescence and the engulfment of new fluid occur.

(vi) During the last observable coalescence of vortex rings, at the end of the transition region, potential-core fluid and some fluid originally contained in the vortices is ejected outwards between the vortices and forms a diffuse, obscuring layer of smoke at the outer part of the jet.

(vii) Regions of diffuse smoke move as coherent structures in the turbulent region. The structures of these large turbulent eddies and their movements are more disorganized than those of the transitional vortex rings.

3.2. *Flow visualization in submerged water jet*

Flow visualization of the transitional and turbulent flows is simplified by using water rather than air because of the lower velocity required to achieve a given Reynolds number. Hydrogen-bubble visualizations of the transitional flow in a 50·8 mm diameter water jet were made for a range of Re. Figure 7 (plate 1) shows a typical frame from a ciné film for $Re = 9000$. Two vortices are coalescing at the end of the transition region and the remains of the previous pair of coalescing vortices can be seen in the turbulent region as a relatively disorganized, diffuse region of bubbles on the right-hand side of the frame. These diffuse regions generally remained observably coherent for several nozzle diameters downstream of the end of the transition region. Thus large eddies in the turbulent jet can be formed directly from the interaction of the transitional vortex rings. As with the smoke jet visualizations, these eddies were much less clearly observable than the vortex rings in the transition region.

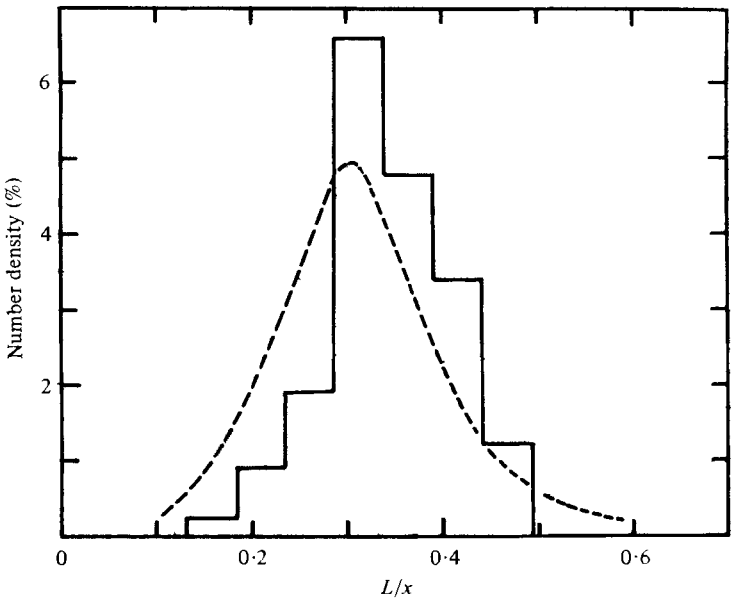

FIGURE 8. Probability distributions of vortex spacings: ——, transitional round jet, $x/D = 1$, $Re = 12000$; – – – –, two-dimensional mixing layer of Roshko (1975).

The movements of vortices in the transition region were measured from the ciné films. The structures of individual vortices and their movements during the coalescing process were neither strictly repetitive nor periodic. For example, although coalescing of the transitional vortices usually involved pairs of vortices, approximately one in six vortex coalescences involved three vortices and less frequently a single vortex stretched and disintegrated, without coalescing.

There is a significant random variation in the process of coalescence. For example, figure 8 shows the probability distribution of the distances between 100 pairs of coalescing vortices as they pass $x/D = 1$ for $Re = 12000$. Figure 8 includes the distribution of vortex spacings in a two-dimensional mixing layer measured by Roshko (1975) and these curves have some similarity. Roshko proposed that his mixing layer was a turbulent flow produced by the random motions of line vortices. However the region in which the present measurements were made in the round jet was not fully turbulent according to the criteria described above. Thus it cannot be said, on the basis of these data, that the random movements of vortex rings effectively produce turbulent flow in a round jet. The differences between the transitional vortex-ring flow and the fully turbulent flow are most clearly realized by studying the three-dimensional nature of the flow as described below.

3.3. *Growth of three-dimensionality during transition*

The interactions of vortex rings during transition produce outward jets of fluid. This fluid forms a relatively diffuse region at the outer part of the jet which moves more slowly than the vortices. This phenomenon is related to the three-dimensional instantaneous structure in the transitional and turbulent flows. As the u, v and w fluctuating velocity components are of the same magnitude in the turbulent region the

instantaneous structures of the transitional and turbulent flows should be investigated in all three dimensions. Understanding the physical processes which occur during the growth of three-dimensional flow is the key to understanding both the nature of the late transitional processes and the essential differences between the turbulent large eddies and vortex rings.

The development of three-dimensional flow in the smoke-filled air jet was investigated by filming the jet looking upstream with cross-sections of the jet at different longitudinal positions illuminated. These films revealed that the growth of three-dimensionality in the transition region was basically an ordered growth of wave deformations of the cores of the vortex rings. Figure 9(*a*) (plate 1) is a front view of the jet with $Re = 10^4$ showing a cross-section at $x = 3D$. This is a section through the trailing edge of the coalescing vortices at the end of the transition region. The fluctuating velocity field at this value of x has not yet attained all the properties of the fully developed turbulent flow, which begins at $x \approx 4D$. Jets of fluid are shed from regions between vortices, as seen in figure 9(*a*). These outward jets form the outer diffuse regions of smoke noted in side views of the jets.

The orderly lobed appearance of the smoke is attributable to the displacement of the vortex core (or coalescing cores) both radially and longitudinally into a standing wave pattern. The films showed that vortices were axisymmetric when they were formed near the nozzle and the amplitude of the wave deformation of the cores then increased with increasing x. This type of natural core instability has been investigated for single impulsively formed vortex rings by Widnall & Sullivan (1973). For a given toroid diameter the number of core waves was found to increase with decreasing thickness of the viscous core. The similarity between the core wave instability in the transitional vortices in the jet and the instability of a single vortex ring can be seen by comparing figure 9(*a*) with figure 9(*b*) (plate 1), which is a front view of a single vortex ring $8D$ from a 50·8 mm diameter nozzle. The vortex has a convection velocity of 3 m/s and thus has similar dimensions and convection velocity to the rings in figure 9(*a*). The circumferential waves in the outer potential flow of the vortices, as marked by the smoke, are in antiphase with the displacement of the vortex core.

The growth of three-dimensionality of the flow, and the loss of circumferential coherence of the initial vortex rings, is also demonstrated by measuring the correlation between velocity fluctuations at circumferentially separated positions. Figure 10 shows measurements of the cross-correlation coefficient for u fluctuations at diametrically opposite points of the mixing layer at $\eta = 0$ for two values of Re. There is seen to be a gradual decrease from the high values near the nozzle, due to the vortex rings, to the low value in the turbulent mixing layer. As is described below, the large turbulent eddies contribute greatly to the velocity fluctuations, so that the low circumferential correlations indicate that the turbulent large eddies are three-dimensional. The growth of core waves in the transitional vortex rings was seen in all the jets studied, up to a 50 mm diameter jet operating at choked conditions and visualized by using the schlieren technique. This phenomenon can also be discerned in previous published visualizations, e.g. those of Bradshaw, Ferriss & Johnson (1964).

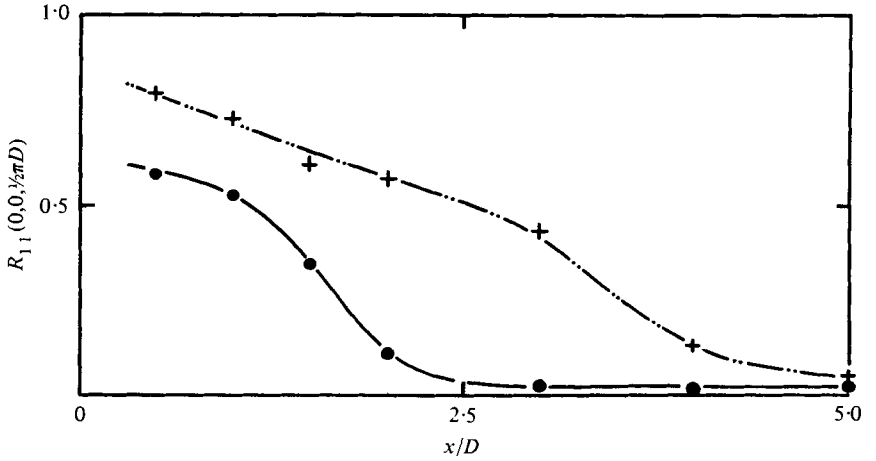

FIGURE 10. Cross-correlation of u at diametrically opposite sides of jet at $\eta = 0$. +, $Re = 9 \times 10^3$; ●, $Re = 3{\cdot}5 \times 10^4$.

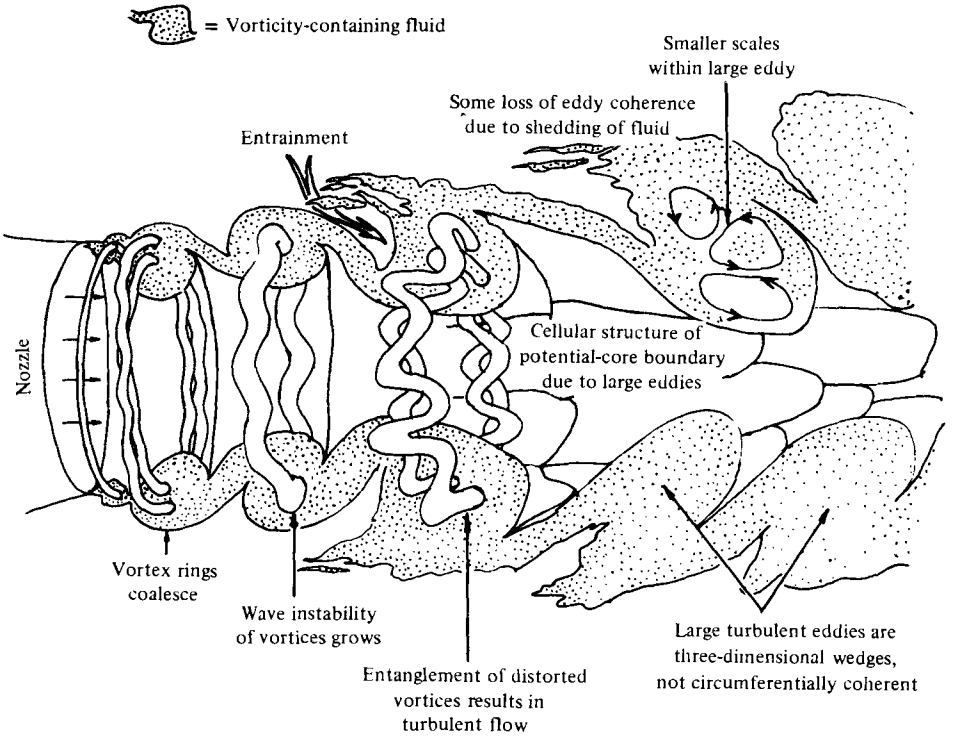

FIGURE 11. Physical structure of transitional jet.

3.4. *General description of transitional jet structure*

The experiments outlined above allow a qualitative description of the events involved in the transition process and these events are sketched in figure 11. Natural instability of the initial laminar shear layer produces a street of vortex-ring-like vorticity concentrations. As these vortex rings move downstream they generally coalesce with

neighbouring rings, so that the scale and separation of the vortex rings increase with distance from the nozzle. However, although point velocity measurements in this transitional flow exhibit periodic correlations and peaked spectra, there is considerable random variation in the movements and strengths of the coalescing vortices. Furthermore the vortex rings lose their phase agreement across the jet as they move downstream. The gradual increase of w fluctuations with distance from the nozzle is caused by the gradual, almost linear, growth of orderly wave deformations of the cores of the vortex rings, and this growth also results in a decrease in the level of circumferential cross-correlations.

From one up to at least three regions of vortex coalescence can be observed in the transition region, depending on the jet Reynolds number and nozzle boundary-layer thickness. Vortex-ring coalescence cannot be observed downstream of the end of the transition region. The coalescing of the vortices is a mechanism by which the jet structure tends to 'forget' the conditions at the jet nozzle. This is evident in figure 6, which shows that the wide range of Strouhal numbers near the nozzle tends to a Reynolds number independent distribution with increasing x.

The last coalescence of vortices, prior to turbulent flow, involves vortex rings which have core deformations larger than a critical size. These rings entangle, thus producing enhanced vorticity stretching and small scales of motion. The remains of these entangled vortices are often visible in the turbulent region up to $5D$ downstream of transition and they are thus large eddies in the turbulent region.

4. Large eddies in turbulent region

4.1. *Flow visualization of turbulent mixing layer*

Injection of dye into the mixing layer near the nozzle in the water jet provided visualization of deformations of the mixing-layer interface produced by large eddies in the fully developed turbulent region. These visualizations were similar to those derived by Dimotakis & Brown (1975) for high Re turbulent two-dimensional mixing layers in a water channel. The dye had a relatively disordered and diffuse appearance at the outer edge of the mixing layer but there was a sharp convoluted interface at the inner, high velocity edge. The bulges of dye at the inner edge, marking the large eddies, have wedges of engulfed potential-core fluid between them similar to those between vortices in the transition region. The entrainment wedges slope backwards at approximately 45° to the axial direction at the centre of the mixing layer. These wedges are the 45° structures evident in many schlieren studies of turbulent jets.

Films of the turbulent regions of both the air and the water jets showed that the large eddies had a wide range of sizes and trajectories at any position and that there was no obvious symmetry between structures on opposite sides of the jet. This again indicates that the eddies lack the circumferential coherence of the transitional vortex rings. Unlike the case of the transition region, apart from the clear interface at the inner, high velocity side of the mixing layer, the visualization of these large eddies was not clear enough to permit a judgement of whether growth in eddy scale was achieved by coalescence. However the observed disappearance of the potential-flow entrainment wedge between adjacent eddies as they moved downstream was an indication of some form of merging process. Intermittent outward jets of dye-

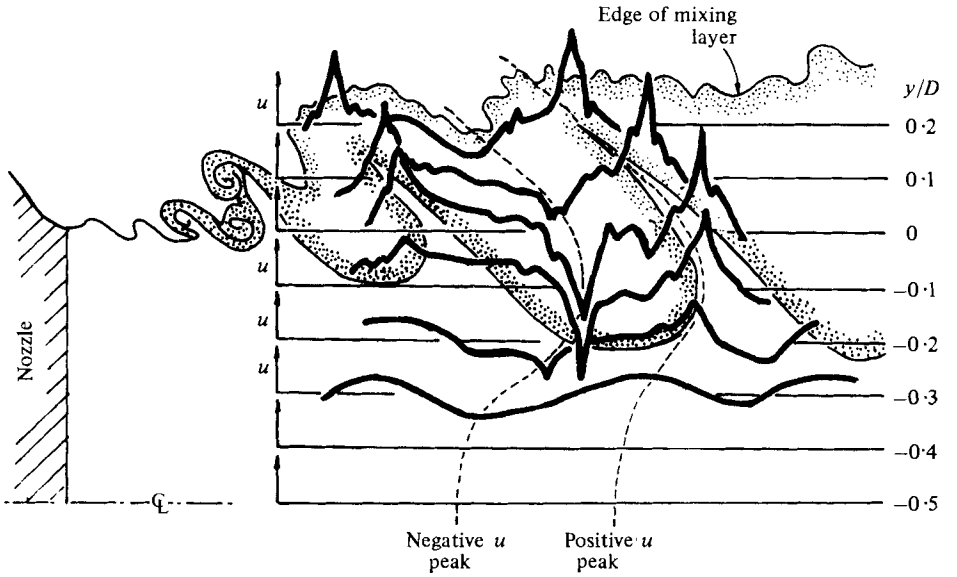

FIGURE 12. Time histories of velocity measured by array of probes in turbulent water jet.

containing fluid burst from the mixing layer. These outward jets appeared to accompany the coalescing process and were similar to the outward jets seen in between vortices at the end of the transition region (figure 9*a*). Visualizations of the jets downstream of the potential core exhibited similar outward bursts of fluid.

4.2. *Derivation of triggering criteria for conditional sampling*

Flow-visualization techniques do not appear to be capable of providing quantitative data on large-eddy structure and interaction in the turbulent region. Thus a conditional sampling technique was developed to study the eddies in more detail. Conditional sampling requires a triggering or conditioning criterion which is directly associated with the event or structure which is to be measured. The selection of suitable triggering criteria, derived from u fluctuations, was facilitated by simultaneously recording velocity time histories while filming the water jet with dye injection. Figure 12 shows u time histories measured by an array of hot wires at different radial positions at $x = 2D$ for $Re = 50\,000$. The flow was locally fully turbulent. The u measurements, shown on arbitrary scales, indicate the relationship between features of these signals and the shape of the edges of the mixing layer as indicated by the dye.

This type of analysis was made for a series of consecutive large eddies. There were considerable variations in the shape of the dye interface and the associated u time histories from one eddy to the next. Usually large peaks in the u signals were found to be the features which could be most easily correlated with the shapes of dye patterns from visual scans of u time histories. These peaks ranged in magnitude from 1·5 to 3 times the local r.m.s. value of u. Thus, at the outer edge of the mixing layer, a series of large positive u peaks was found and these corresponded to regions of dye projecting from the jet. In the centre of the mixing layer both large positive and large negative peaks were found while at the high velocity edge of the mixing layer large negative u

peaks corresponded to regions within the eddies. As is indicated in figure 12, the positions of both the negative and the positive u peaks advance and then retreat in phase as one moves out from the centre of the jet. In the central part of the potential core, positive peaks in the u fluctuations roughly corresponded to the passing of the bulge of dye marking the large eddy and negative peaks corresponded to the interval between eddies passing.

Examination of the hydrogen-bubble time lines in figure 7 shows a similar relation between potential-core u fluctuations and the passing of transitional vortices. However, the u fluctuations outside the potential core were quite different for the turbulent and transitional vortex-ring cases. The axisymmetric vortex rings at the beginning of the transition region produced skewness in u fluctuations but with opposite sign to that produced by the large turbulent eddies. This was because the initial vortices contained relatively thin viscous cores with high angular velocities, so that velocity overshoots occurred at the edges of the cores. On the other hand the turbulent eddies appeared to approximate, in cross-section, to wide regions of smaller-scale turbulence undergoing a slow solid-body rotation. Thus the vortex rings produced large negative u peaks at the outer edge of the mixing layer (sometimes producing reverse flow) and large positive u peaks at the inner edge, where the instantaneous velocity exceeds U_j by up to 20 % in the transition region but by never more than 2 % in the turbulent region. In the transition region vortex rings produced smooth low frequency velocity variations with larger gradients as the viscous cores passed. A detailed study showed that the vortex rings had basically similar structures to classical single vortex rings with cores of solid-body rotation. Bruun (1977) has used conditional sampling techniques to measure averaged vortex structures in this region, but did not differentiate between the inner and outer vortices of the clearly seen coalescing vortex pairs.

In the turbulent region it was found that, although smooth velocity signals were measured in potential-flow regions, the flow in the dye-containing, rotational regions of the eddies produced higher frequency, lower amplitude u signals superimposed on the basic large amplitude peaks. These higher frequencies represent the smaller scales of turbulence and can perhaps be considered physically as the interacting remnants of smaller eddies and vortices which merged at earlier times.

4.3. *Conditional sampling of large eddies in turbulent mixing layers*

An extensive study has been made of the relationships between large u and v peaks and large-eddy structure and the use of these peaks to conditionally sample the large eddies in the turbulent jet. Parts of this work will be reported at a later date. It was found (Yule *et al.* 1974) that the large positive and negative u peaks occur at similar times to large peaks in v. Thus the movements of fluid induced by the large eddies, which are responsible for these peaks, provide the major contribution to the shear stress $\overline{uv}$. Conditional sampling using the large u peaks near the centre of the mixing layer enabled the derivation of radial phase variations and the convection of the flow structures downstream; see Lau & Fisher (1975) and Yule *et al.* (1974). However the large variations in eddy structure and movement at any position resulted in recovered signals with very low levels. Conditional sampling of a particularly repetitive type of eddy will produce a recovered signal with a reasonably high level and an experiment of this type is described below.

There is evidence that a coherent large-scale structure in the jet mixing layer is most likely to be found between the centre and the inner, high velocity side of the mixing layer. In addition to the present flow visualizations, Browand & Laufer (1975) and Crow & Chamagne (1971) have noted the irregular appearance of the outer part of the jet. Ko & Davies (1971), and others, have deduced that the major source of pressure fluctuations in both the near field and the potential core of the turbulent jet is centred at the inner side of the mixing layer. Thus it is to be expected that a conditional sampling technique is most likely to be successful if it is applied to the inner side of the mixing layer. The technique described below selects those eddies on the inner side of the mixing layer which move very close to the jet centre-line. This procedure greatly reduces the 'smearing' of recovered signals caused by the range of eddy trajectories. It should be noted that, if the magnitude of the recovered signals in this type of conditional sampling procedure are not large in comparison with the covariance between the signals of the triggering and the recovery probe, the conditional sampling method offers little more information than the classical correlation technique and is thus not worthwhile.

The combined flow-visualization/hot-wire experiment showed that when a turbulent eddy moved unusually close to the jet centre-line the local potential-core u fluctuations had unusually large positive and negative peaks. The probe positions used for conditional sampling are shown in figure 1. The triggering hot-wire probe, measuring u_1, was positioned in the air-jet potential core at $x = 2D$, $\eta = -0{\cdot}2$ for $Re = 43\,000$. Previous experiments showed that there was fully developed turbulence for $x \geqslant 2D$. When u_1 had a negative peak with a magnitude greater than $2{\cdot}8\,(\overline{u^2})^{\frac{1}{2}}$ an electronic triggering circuit was activated and the subsequent 0·01 s of u_2 time history at the recovery probe was measured and stored. The final conditionally sampled signal u_s was derived by obtaining an ensemble average of at least 256 portions of the u_2 time history by using 256 consecutive large u_1 peaks. These triggering peaks represent 5 % of the total u_1 negative peaks and thus one can assume that roughly 5 % of the total number of large eddies responsible for the potential-core fluctuations were sampled.

Figure 13 shows the conditionally sampled time histories of the fluctuating velocity components u_s and v_s at $x = 2{\cdot}5D$. The large negative u_s peaks at $\eta = -0{\cdot}15$ and $\eta = -0{\cdot}1$ correspond to the triggering peak, which has been convected downstream from $x = 2D$. The large negative u peaks in the potential core are seen to correspond to structures producing positive u peaks in the centre and outer parts of the mixing layer and both large negative and large positive v peaks for the complete width of the mixing layer. Similar measurements at larger values of x showed that these sampled signals retained their shapes up to the end of the potential core ($x = 6D$) and had a convection velocity $U_c = 0{\cdot}72U_j$ for $-0{\cdot}2 < \eta < 0$. The v_s signals retained 75 % of their magnitude at the end of the potential core but the magnitude of the u_s signal dropped to approximately 40 %. Thus v-component distributions associated with the sampled eddies were more coherent than the u distributions both spatially and with increasing existence times of the eddies.

Figure 14 shows that the magnitudes of the sampled signals are comparable to local r.m.s. signals and larger than would be expected from the measured statistical covariance between the signals at the triggering and recovery probes. One can thus conclude that a repetitive class of eddy is being sampled which retains its coherence

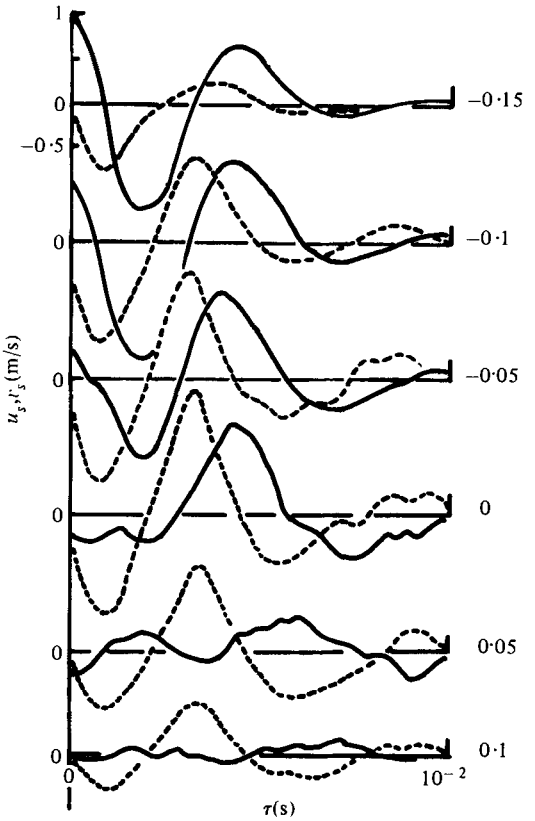

FIGURE 13. Conditionally sampled time histories of u and v at $x/D = 2{\cdot}5$, $Re = 4{\cdot}3 \times 10^4$. Triggered by negative u_1 peaks greater than $2{\cdot}8(\overline{u_1^2})^{\frac{1}{2}}$ at $x/D = 2$, $\eta = -0{\cdot}2$. ——, u_s; – – – –, v_s.

at least to the end of the potential core, is coherent for most of the width of the mixing layer, and is responsible for particularly large velocity fluctuations in the potential core.

The sampled signals at different values of x showed that, for longitudinal distances up to about $1{\cdot}5D$ from the triggering position, it was reasonable to invoke the Taylor hypothesis of an unchanging convected eddy structure for the sampled eddies. Thus the u_s and v_s time histories at $x = 2{\cdot}5D$ were converted into an approximate spatial velocity field in a co-ordinate system moving with the velocity $U_c = 0{\cdot}72U_j$. In this moving frame of reference the transverse velocity component is v_s and the longitudinal velocity component is given by $U + u_s - U_c$. Figure 15 shows the directions and magnitudes (given by the length of each arrow) of the local velocity for the sampled eddies moving in this frame of reference. It is seen that the large negative u triggering peaks occurred between two large eddies on the inner side of the mixing layer which were on average $1{\cdot}3D$ apart at $x = 2{\cdot}5D$. The general form of the cross-sections of the sampled eddies, with their longitudinally elongated cores, is very similar to that of laminar vortex rings. However, as has been described, these eddies are not axisymmetric.

The conditional sampling technique inherently averages, and thus conceals, any randomness associated with the eddies. Thus although u and v fluctuations with higher frequency components than those associated with the large-eddy scale are known to be present within the eddies, they are concealed by the sampling technique, which

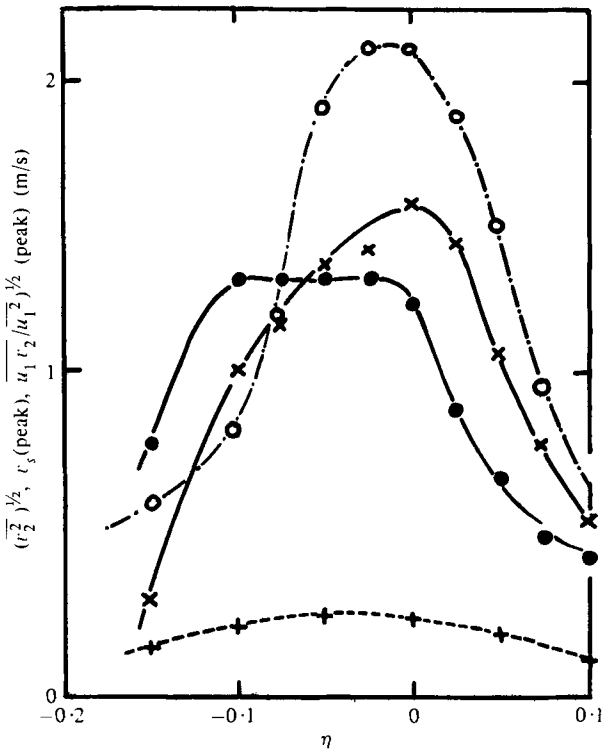

FIGURE 14. Distribution of radial intensity component $(\overline{v_2^2})^{\frac{1}{2}}$ at $x/D = 2{\cdot}5$ compared with peak values of conditionally sampled signals v_s and peak values of covariance $\overline{u_1 v_2}$ between trigger and recovery probe signals (divided by r.m.s. of u_1). ○, $(\overline{v_2^2})^{\frac{1}{2}}$; ×, v_s, positive peak; ●, v_s, negative peak; +, $\overline{u_1 v_2}/(\overline{u_1^2})^{\frac{1}{2}}$, peak value.

produces the orderly velocity field seen in figure 15. The spatial phase variations of the u and v peaks associated with the sampled eddies are included in figure 15. It is seen that the sampled u and v signals appear to be approximately in quadrature for much for the width of the jet and this implies that there is little contribution to the shear stress $\overline{uv}$ by the sampled eddies. However, examination of the u_s and v_s time histories at different radial positions (figure 13) shows that asymmetries in these signals give small net positive contributions to the shear stress. It appears that the sampling technique is measuring an inner component of the coherent large eddies and that other components, probably in the outer part of the mixing layer, are not important contributors to the large potential-core fluctuations and are thus not measured. The interaction and merging of the sampled structures with other components of the motion may thus give important contributions to the shear stress.

As has been noted, there is substantial evidence that the larger scales of motion at the outer side of the mixing layer lack the regularity, coherence and relative repetitiveness of the large eddies in the inner region. This appears to be an additional fundamental difference between the turbulent mixing layer and the early transitional vortex region, which contains coalescing, 'leap-frogging' vortices on both the inner and the outer sides of the mixing layer. Further evidence of a lack of regularity in the outer part of the mixing layer was found in the results of double-triggering experiments,

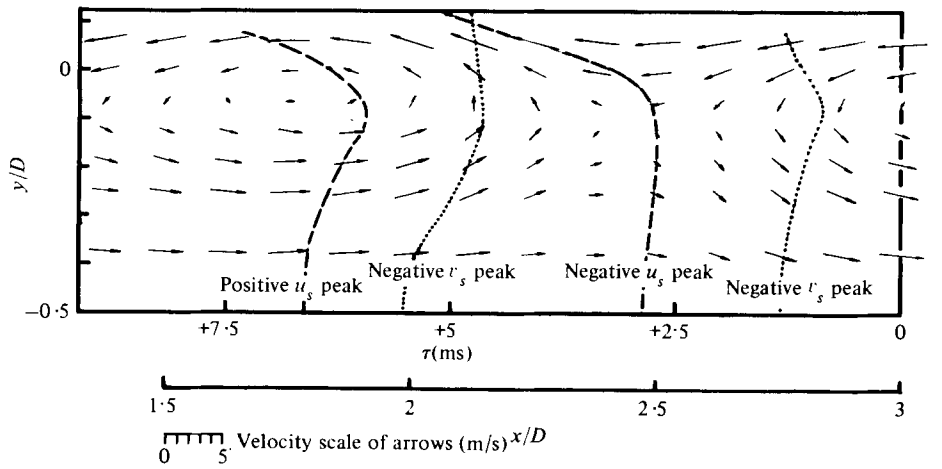

FIGURE 15. Conditionally sampled velocity field associated with large negative u peaks at $\eta = -0{\cdot}2$, $x/D = 2$, $Re = 4{\cdot}3 \times 10^4$.

similar to those developed independently by Browand & Weidman (1976). In these experiments the signal from a third probe in the mixing layer was sampled only when the peaks of u fluctuations in the inner and outer potential flows had a preset phase difference. The results of these experiments are not described as they produced no evidence of an organized structure in the outer part of the mixing layer. The recovered signal was very weakly dependent on the outer trigger signal but was dominated by the inner, potential-core, trigger. Thus only an inner large-eddy component was measured with a reasonable degree of spatial and temporal coherence. This contrasts with the results of Browand & Weidman, which clearly show vortices in both the inner and the outer regions and show the averaged structures of vortex pairs in different stages of coalescence. This double-trigger technique would probably produce similar results to those of Browand & Weidman if it were applied to the transition region of the round jet, where coalescing vortices can be seen clearly. It appears that the flow of Browand & Weidman had more similarities with the early transitional flow in the round jet than with the turbulent round-jet mixing layer described above.

On the basis of these observations it is deduced that the outer region of the mixing layer contains random outward bursts of fluid which apparently orginate from the interaction or disintegration of the inner large eddies. The coherence of these regions of ejected flow is very short lived and they mix with fluid ejected at an earlier time to produce a diffuse irregular structure in the outer region. In common with the structure of the inner large eddies, and unlike the case of the transitional vortices, the structure of the outer region is fully three-dimensional. Thus there is no evidence of significant circumferential coherence of structures, the length scales in the radial and circumferential directions being similar. The coherent large eddies which have been measured are so strong that they are important contributors to correlations and are likely to have an important influence on aerodynamic noise and mixing. However one should not underestimate either the complexity of these eddies and their interactions or the potential importance of the less organized regions of the turbulent flow, which appear to contain a substantial proportion of the mass flow at any axial position and which may also give important contributions to mixing, shear stress and other phenomena.

5. Concluding remarks

The existence of vortex rings in the round jet has been proved conclusively for only a relatively short transitional, Reynolds number dependent, region near the nozzle. These initial vortex rings have been observed to coalesce. However, the region where this is observed is not turbulent. There are substantial differences between the structures of the transitional (vortex ring) region near the nozzle and the fully developed turbulent mixing-layer region. Such differences cannot be reconciled with the existence of axisymmetric vortex rings in both regions. The ease with which coherent laminar-vortex-type structures can be visualized in low Reynolds number transitional or artificially stabilized turbulent flows can lead to the tempting, but often unsubstantiated, use of data for such flows to describe the structures of the fully turbulent regions of the same flows.

It has been shown that transition in round jets can involve the entanglement of streets of vortex rings which have developed wave deformations of their viscous cores. The large-scale structures produced by this process form coherent large eddies in the mixing-layer region. It appears that much of the transitional flow is sufficiently orderly to be amenable to three-dimensional computer modelling. Coherent three-dimensional eddies are such dominating components of the turbulent mixing layer that their structures and interaction are essential aspects of future experimental and modelling studies of the round jet. The structure of the turbulent mixing layers had Reynolds number similarity for the range of jets studied and the physical events occurring during transition were essentially identical for all of the jets.

The experiments were supported by the Science Research Council at the University of Southampton. The author thanks P. O. A. L. Davies, for many useful discussions, H. H. Bruun, whose data are included in figure 5, D. R. J. Baxter, for his aid in photographic studies, and appreciates the helpful comments of P. Bradshaw and N. A. Chigier.

REFERENCES

BRADSHAW, P. 1966 The effect of initial conditions on the development of a free shear layer. *J. Fluid Mech.* **26**, 225–236.

BRADSHAW, P. 1975 In *Turbulent Mixing in Nonreactive and Reactive Flows* (ed. S. N. B. Murthy), pp. 311–312. Plenum.

BRADSHAW, P., FERRISS, D. H. & JOHNSON, R. F. 1964 Turbulence in the noise-producing region of a circular jet. *J. Fluid Mech.* **19**, 591–624.

BROWAND, F. K. & LAUFER, J. 1975 The role of large scale structures in the initial development of circular jets. *Proc. 4th Biennial Symp. Turbulence in Liquids, Univ. Missouri–Rolla*, pp. 333–344. Princeton, New Jersey: Science Press.

BROWAND, F. K. & WEIDMAN, P. D. 1976 Large scales in the developing mixing layer. *J. Fluid Mech.* **76**, 127–144.

BROWN, G. & ROSHKO, A. 1971 The effect of density difference on the turbulent mixing layer. *AGARD Conf. Proc.* no. 93, paper 23.

BROWN, G. & ROSHKO, A. 1974 On density effects and large structure in turbulent mixing layers. *J. Fluid Mech.* **64**, 775–816.

BRUUN, H. H. 1977 A time-domain analysis of the large-scale flow structure in a circular jet. Part 1. Moderate Reynolds number. *J. Fluid Mech.* **83**, 641–671.

CHANDRSUDA, C., MEHTA, R. D., WEIR, A. D. & BRADSHAW, P. 1978 Effect of free-stream turbulence on large structure in turbulent mixing layers. *J. Fluid Mech.* **85**, 693–704.

CROW, S. & CHAMPAGNE, F. M. 1971 Orderly structure in jet turbulence. *J. Fluid Mech.* **48**, 547–591.

DAVIES, P. O. A. L. & YULE, A. J. 1975 Coherent structures in turbulence. *J. Fluid Mech.* **69**, 513–537.

DIMOTAKIS, P. E. & BROWN, G. L. 1975 Large structure dynamics and entrainment in the mixing layer at high Reynolds number. *Project SQUID, Purdue Univ. Indiana, Tech. Rep.* (II-7-PU).

DIMOTAKIS, P. E. & BROWN, G. L. 1976 The mixing layer at high Reynolds number: large-structure dynamics and entrainment. *J. Fluid Mech.* **78**, 535–560.

KO, N. W. M. & DAVIES, P. O. A. L. 1971 The near field within the potential cone of subsonic cold jets. *J. Fluid Mech.* **50**, 49–78.

KONRAD, J. H. 1976 An experimental investigation of mixing in two-dimensional turbulent shear flows with applications to diffusion-limited chemical reactions. *Project SQUID, Purdue Univ. Indiana, Tech. Rep.* CIT-8-PU.

LAU, J. C. & FISHER, M. J. 1975 The vortex-street structure of 'turbulent' jets. Part 1. *J. Fluid Mech.* **67**, 299–337.

LAUFER, J., KAPLAN, R. E. & CHU, W. T. 1973 On the generation of jet noise. *AGARD Conf. Noise Mechanisms, Brussels*, paper 131.

MAXWORTHY, T. 1974 Turbulent vortex rings. *J. Fluid Mech.* **64**, 227–239.

MICHALKE, A. & FREYMUTH, P. 1966 The instability and the formation of vortices in a free boundary layer. *AGARD, Conf. Proc.* no. 4, paper 2.

MOORE, C. J. 1977 The role of shear-layer instability waves in jet exhaust noise. *J. Fluid Mech.* **80**, 321–367.

ROSHKO, A. 1975 Progress and problems in understanding turbulent shear flows. In *Turbulent Mixing in Nonreactive and Reactive Flows* (ed. S. N. B. Murthy), pp. 295–311. Plenum.

WIDNALL, S. E. & SULLIVAN, J. P. 1973 On the stability of vortex rings. *Proc. Roy. Soc.* A **332**, 335–353.

WILLE, R. 1963 Growth of velocity fluctuations leading to turbulence in a free shear layer. *Hermann Fottinger Inst., Berlin, AFOSR Tech. Rep.* Contract AF 61(052)–412.

WINANT, C. D. & BROWAND, F. K. 1974 Vortex pairing: the mechanism of turbulent mixing-layer growth at moderate Reynolds number. *J. Fluid Mech.* **63**, 237–255.

YULE, A. J. 1972 Two-dimensional self-preserving turbulent mixing layers at different free stream velocity ratios. *Aero. Res. Counc. R. & M.* no. 3683.

YULE, A. J., BRUUN, H. H., BAXTER, D. R. J. & DAVIES, P. O. A. L. 1974 Structure of turbulent jets. *Univ. Southampton ISVR Memo.* no. 506.

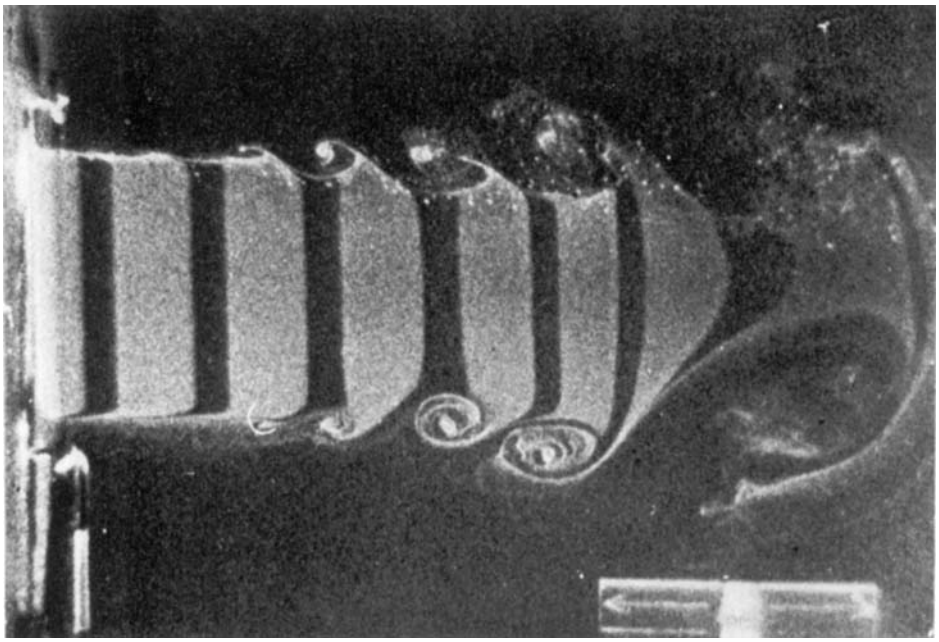

FIGURE 7. Submerged water jet visualized by pulsed formation of hydrogen bubbles across vertical diameter at orifice; Re = 9000.

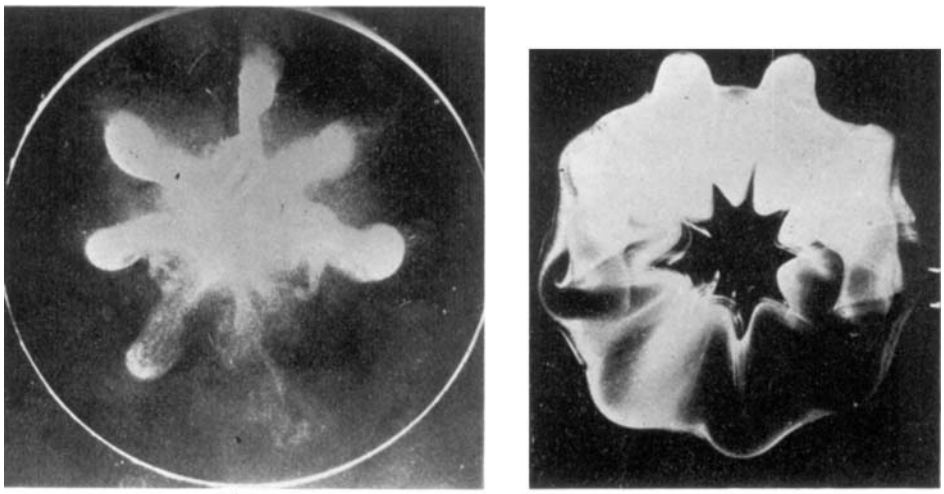

(*a*) (*b*)

FIGURE 9. (*a*) Axial view of cross-section of smoke-filled air jet; $Re = 10^4$, $x/D = 3$. (*b*) Axial view of unstable single vortex ring.